Design, Fabrication, and Uniformity Testing of a Versatile, Low-Cost Student Wind Tunnel

Samuel V. Jett* and Karen Martinez Soto*
University of Oklahoma Aerospace and Mechanical Engineering, Norman, OK, 73019, USA

Orhan Roksa† and Marko Mestrovic†
University of Oklahoma Aerospace and Mechanical Engineering, Norman, OK, 73019, USA

Dr. Thomas C. Hays‡
University of Oklahoma Aerospace and Mechanical Engineering, Norman, OK, 73019, USA

In recent years, research into application and optimization of unmanned aerial vehicles (UAVs) has been growing in popularity. To test full-scale UAV propellers,wind tunnels with large test sections are needed. In addition, some modifications to an existing tunnel are needed, that, for both administrative and technical reasons, would be difficult to add to existing expensive commercial wind tunnels. For these purposes, and to increase student capacity to use wind tunnels, our group designed and fabricated a versatile, low-cost wind-tunnel with a large 36 in square test section for use by student researchers at the University of Oklahoma. We expect that this tunnel will serve aerodynamics researchers by providing a flexible and robust platform for development and testing of many aerodynamics components, including UAV propellers. The following report includes a description of the design and construction processes and preliminary uniformity testing of the tunnel for validation purposes.

I. Nomenclature

A_{in}	=	Cross-sectional area of velocity inlet boundary condition
A_{TS}	=	Cross-sectional area of the test section
P_{atm}	=	Atmospheric pressure
P_{TS}	=	Estimated pressure in test section under normal operation
V_{in}	=	uniform velocity inlet boundary condition for CFD analysis
V_{TS}	=	the predicted flow velocity in the test section (60 ft/s)
ΔP	=	Pressure difference between internal test section and atmosphere
ρ_{air}	=	Density of air

II. Introduction

Wind tunnels are a commonly utilized tool in aerodynamics research. Tunnels generate a uniform flow field with known flow velocity and pressure and allow the precise quantification of a solid body's interaction with external air flow [1]. Although other aerodynamics study tools exist, namely simulations employing computational fluid dynamics (CFD), precise measurement of flow patterns, and parameters like flow velocity, pressure, and solid deformation or displacement within a properly sized wind tunnel remains the ideal method for determining external flow characteristics [2]. The Department of Aerospace and Mechanical Engineering (AME) at the University of Oklahoma (OU) currently utilizes and maintains a number of wind tunnels, predominantly for research use, but also for student use in laboratory courses. However, these tunnels were costly to purchase, and because of this cost are of limited availability for student experimentation. In addition, the precision of commercial wind tunnels like these frequently dissuades researchers from attaching custom-built parts to the tunnel, and from making research-driven modifications to the tunnel, because of

*Undergraduate Student. Department of Mechanical and Aerospace Engineering, AIAA Student Member
†Undergraduate Student. Department of Mechanical and Aerospace Engineering
‡Assistant Professor. Department of Mechanical and Aerospace Engineering, AIAA Professional Member

concerns for damaging the flow quality in the tunnel.

Recently, researchers have examined the application of unmanned aerial vehicles (UAVs) toward many data-acquisition endeavors in fields like meteorology, agriculture, traffic surveillance, and more [3–6].These UAVs frequently utilize a propeller driven design, whether in a vertical, "copter" configuration (air driven downward) or a horizontal, "plane" configuration (air driven backward). To reduce the power required and to increase the efficiency of propeller-driven UAVs, consideration of the propeller utilized in the expected flow conditions is required [7, 8]. To examine the torque generated and the revolution rate of propellers in a specified flow rate, propellers can be mounted to a dynamometer and driven by the known flow conditions. However, non-purpose-built wind tunnels cannot accommodate the size of needed propellers (diameter 6 inches to 28 inches), nor the attachment of a dynamometer to allow these measurements to be taken [9]. In addition, CFD trials to characterize the efficacy of propeller design are computationally costly to operate and frequently struggle to capture the effects of minor changes in propeller design [10]. Therefore, wind tunnels that can accommodate the size of full-scale propellers (estimated up to 28 in diameter for most applications) and the attachment of a dynamometer are necessary to validate and improve design of UAVs.

Our group designed, fabricated, and conducted uniformity testing on a low-cost multipurpose wind tunnel with capacity to test UAV propellers. We examined flow characteristics for open and closed loop wind tunnels, through use of computer-aided design (CAD) models and testing with CFD methods. Our design took a manufacturability and budget-centered approach while ensuring that the tunnel met necessary performance parameters, particularly in test-section size, overall tunnel size (location constraints), and power source constraints. After settling on a design, we manufactured the tunnel with mainly low-cost materials at fabrication facilities made available through OU. To explore the uniformity of the flow within the test section, we conducted brief testing using a hot-wire anemometer and analyzed the flow speed on a nodal basis throughout the cross-sectional area of the tunnel test section.

III. Methods

This section details the design process utilized by the wind tunnel team, the fabrication methods used by the team, and the procedures used in the flow uniformity study. In the design process, it is important to understand the limitations that our team faced initially. We were initially required to design and build the wind tunnel to operate in a room with dimensions 19 ft long by 17 ft wide by 8 ft tall. We also had no access to three-phase power, and although we could pay for a three-phase outlet to be installed in the wind-tunnel room, our funding was limited to $5000. Thus, we chose not to invest in three-phase power. We also looked at using an engine to power our motor but were unable to pursue this option due to noise constraints. Without spending more than half of our budget on electrical modifications to the room, we were essentially limited to an estimated two horsepower from the standard electrical outlets. Therefore, our three primary limitations were room size, budget, and power. We ended up overcoming the first and last barriers by finding a new location for the wind tunnel with more relaxed noise requirements, but most of the design stage was performed with the assumption of these three constraints.

A. Wind Tunnel Design and CFD Testing

Wind tunnels can be broadly divided into two categories: open-loop tunnels, where the air is constantly exhausted and new air inhaled, and closed-loop tunnels, where the same air is continuously recycled. The decision of what tunnel type to pursue underlay all future design decisions, so our group addressed this question first. Initially, we pursued a closed-loop model because we were constrained by the amount of power we could use and the space we had to build the tunnel. Our principal designs and analyses of the closed-loop design are shown in Fig. 1 below. We were required to keep the tunnel relatively short, to allow it to fit in a 19 ft long room. In addition, we were limited in the number of horsepower we could draw from a standard outlet, so we initially chose to pursue the closed-loop design because of the lower power requirements to produce test-section velocities in the range of 50 ft/s and because it required a shorter diffuser section. For all CFD testing, the driving fan was simulated through a uniform velocity inlet boundary condition, based on the maximum predicted velocity in the test section and the cross-sectional area ratio between the test section and the outlet. This formula, based upon the conservation of volumetric flow rate, relies upon the incompressibility of air in low velocity applications ($V_{TS,max} < 60$ ft/s).

$$V_{in} = V_{TS,max} \frac{A_{TS}}{A_{in}} \tag{1}$$

The BC opposite the velocity inlet was modeled as an atmospheric pressure inlet on the face directly upstream of the velocity output. These CFD trials served our purpose of revealing the extent of flow uniformity in the test section rapidly

while remaining simple to implement.

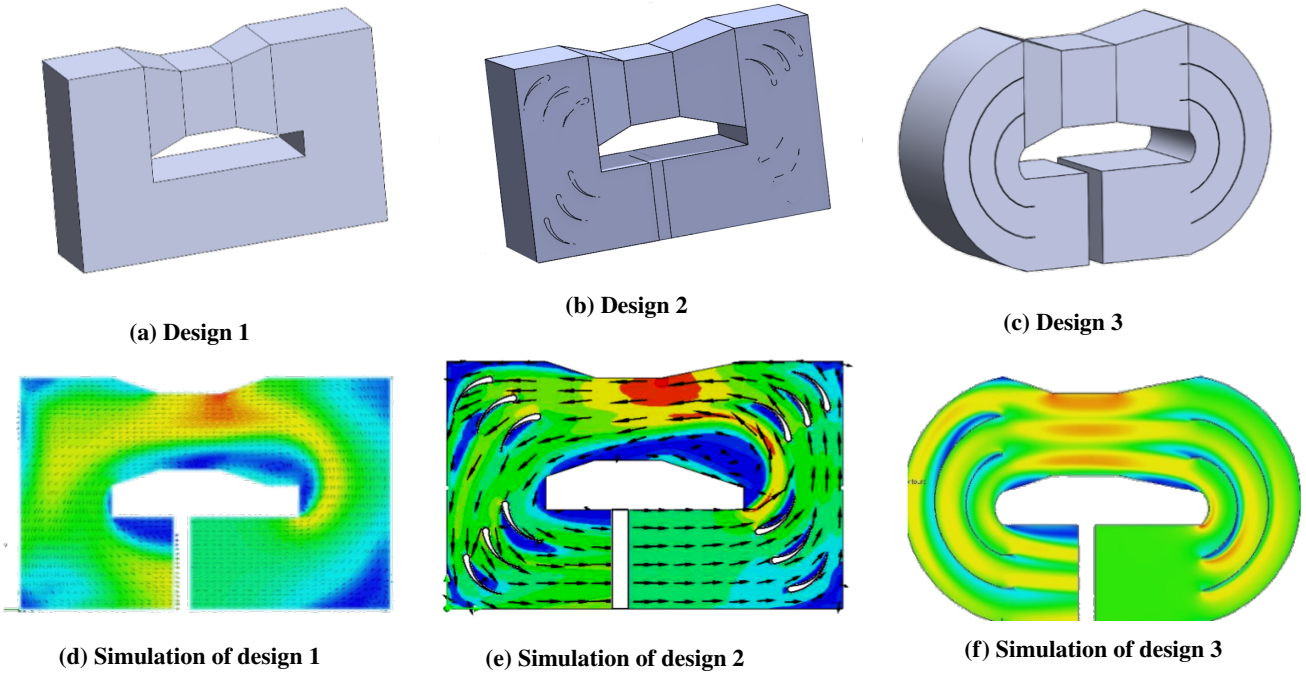

(a) Design 1 **(b) Design 2** **(c) Design 3**

(d) Simulation of design 1 **(e) Simulation of design 2** **(f) Simulation of design 3**

Fig. 1 Three CAD designs for the closed-loop wind tunnel. Tunnels were designed in SolidWorks (SW) with included CFD flow results generated by Flow Simulation with test section velocities of approximately 60 ft/s

For all three closed-loop designs, the test section was located at the top of the tunnel, and the empty gap shown in the lower half of the tunnel was designed to allow the applied pressure and velocity BCs to be applied, in lieu of a fan. The flow direction is shown in Fig. 1e. Our closed-loop designs, even with the addition of turning vanes (Fig. 1a, c) and other modifications, were unable to produce uniform flow in the test section(Fig. 1d, f). To remedy this, we attempted to implement a honeycomb flow-straightener into our CAD model and simulations but were unable to implement the screen into CFD simulations because of meshing issues with the small size of the screens [11, 12]. Design of the flow-straightener is included in the Appendix (Fig. A1). Because of this issue with flow uniformity and the expected difficulty of manufacturing the closed-loop wind tunnel we began to consider open-loop designs. Our initial open-loop prototype and its respective CFD simulation are shown below in Fig. 2.

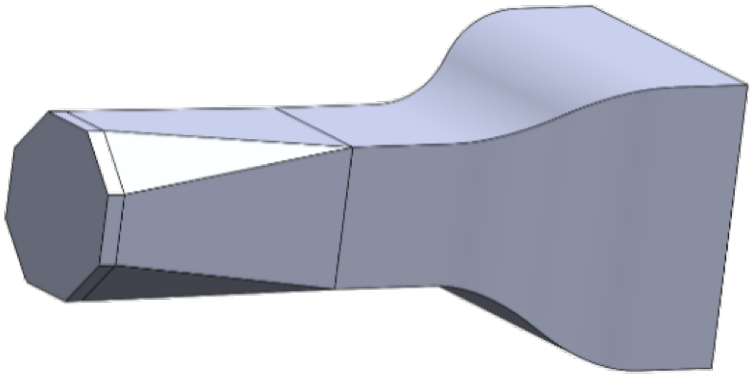

Fig. 2a Initial CAD prototype of open-loop tunnel

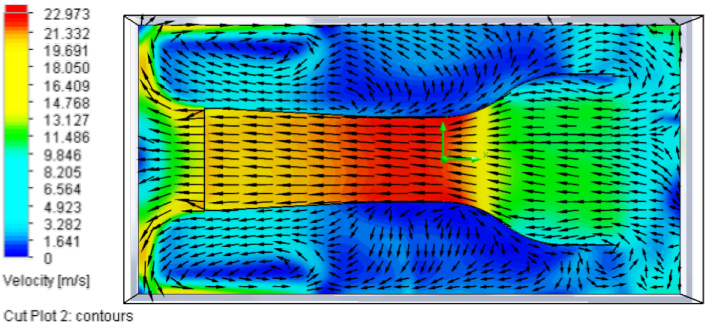

Fig. 2b Initial CFD simulation of open-loop tunnel

The open-loop tunnel was designed for manufacturing using plywood panels fit to contours defined by Hernandez et al. [13].Through CFD testing with the same BCs applied to model our driving fan, we noted that the open-loop prototype produced a more uniform flow field than the closed-loop designs. Still, we noted some variance in the flow direction within the test-section, and dead zones in the contraction, belying the need for a redesigned contraction. Despite these issues, the open-loop tunnel showed promise for functioning in the confined space. With the CFD results and open-loop analysis completed, we designed a more supported and robust CAD model to advise construction. Changes were made to the structure of the contraction to eliminate the dead zones and pyramidal diffusers were added to the inlet and outlet of the tunnel to promote smooth flow entry and exit. Structurally-supportive beams were also added to the model. The final design was broken into four sections: contraction, test section, tunnel diffuser, and wall-mounted diffusers (Fig. 3).

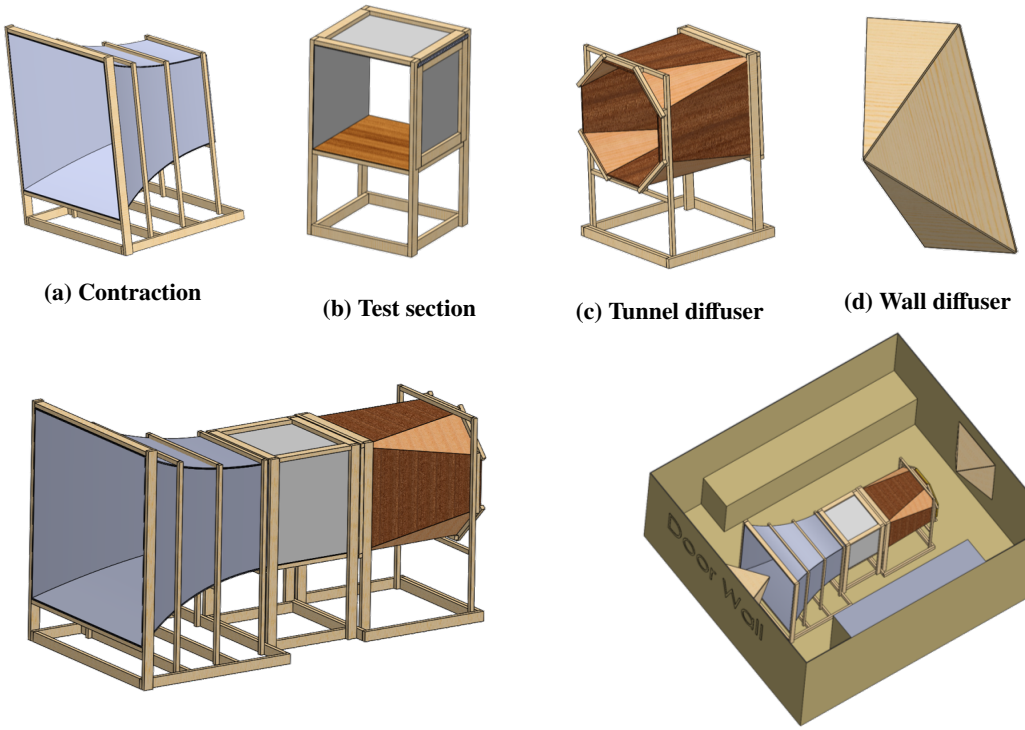

(a) Contraction **(b) Test section** **(c) Tunnel diffuser** **(d) Wall diffuser**

(e) Completed tunnel **(f) Anticipated tunnel placement**

Fig. 3 CAD models of the wind tunnel

Various testing was performed on this tunnel design. In addition, we performed a static-structural finite element analysis (FEA) on the acrylic sheets used to enclose the test section. Briefly, we used Bernoulli's principle to calculate the pressure loads on the sheet, assuming a test section flow velocity of 60 ft/s, and then conducted FEA using ANSYS software to examine the deformation of the acrylic sheet. The pressure inside the test section is shown below as a function of the test section velocity and the pressure and density of air.

$$P_{TS} = P_{atm} - \rho_{air} \frac{V_{TS}^2}{2} \tag{2}$$

The pressure applied uniformly across the door in the static-structural analysis was then defined as the pressure gradient between the test section pressure and atmospheric pressure, as shown below.

$$\begin{aligned} \Delta P &= P_{atm} - P_{TS} \\ &= \rho_{air} \frac{V_{TS}^2}{2} \\ &\approx 4.28 \quad \text{psf} \end{aligned} \tag{3}$$

The acrylic sheet and the testing results are shown in the Appendix in Fig. 10. Analysis showed that even a thin (0.25 in) acrylic sheet should handle the pressure loading without buckling. Flow testing results from a variety of viewing angles are shown in Fig. 4 below. The CFD tests shown were performed in the same manner as before with both a velocity inlet BC on the tunnel face of the diffuser and an atmospheric pressure outlet BC downstream of the tunnel diffuser.

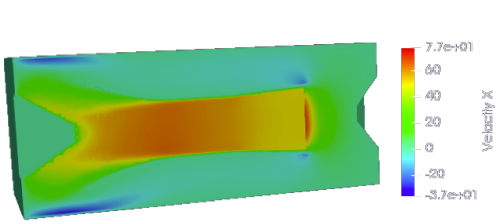

(a) Side view of flow

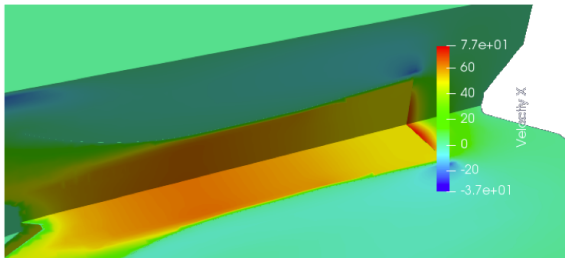

(b) Isometric view of flow

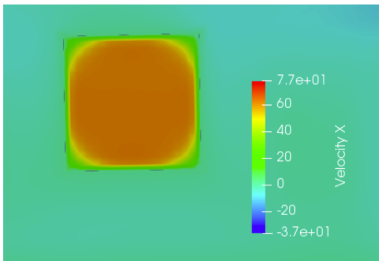

(c) Cross-section of flow

Fig. 4 CFD testing for the design displayed in Fig. 3e

Given the favorable results of CFD testing, we were planning to utilize the design shown in Fig. 3e for our tunnel build. However, at this point we were given access to a new room to house our tunnel, with no sound requirements, allowing the use of an engine and a larger tunnel. So, we scaled the design shown in Fig. 3e, and added further structural supports. In particular, we thought it would be beneficial to increase the cross-sectional area of the test section to a 3 ft square, and to lengthen the diffuser, to ensure the flow remained attached to the diffuser walls [13]. We also eliminated the wall-mounted diffusers, due to the larger room provided. These modifications and the addition of the fan to the tunnel were aided by faculty sponsor Thomas Hays, Ph.D. The modified tunnel, adopted as our final design, is shown in Fig. 5 below.

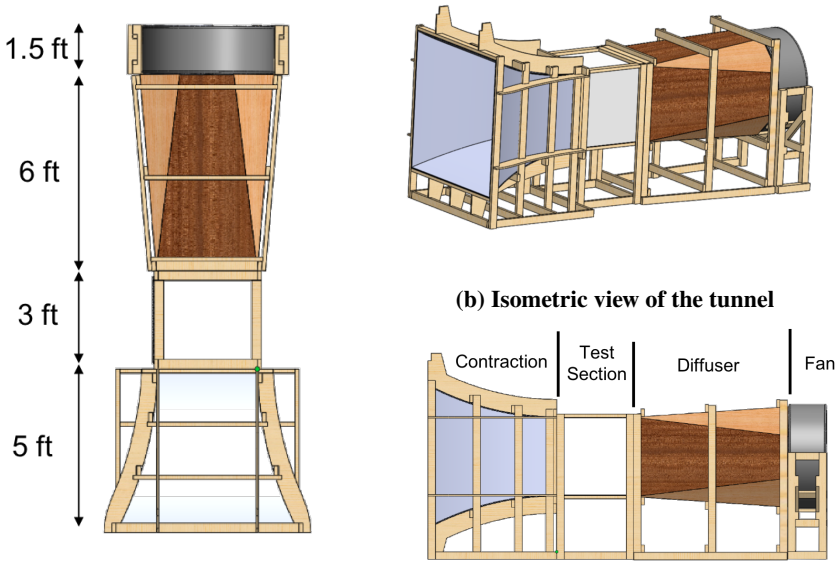

(a) Component lengths

(b) Isometric view of the tunnel

(c) Tunnel sections labeled

Fig. 5 CAD models for final wind tunnel design

This final design was constructed in pieces in the AME machine shop, using standard pine 2x4 struts and $\frac{3}{4}$ inch pine plywood sheets for the diffuser and the base and roof of the test section. Acrylic of thickness $\frac{1}{2}$ inch was used for the sidewalls of the test section, and two layers of $\frac{1}{4}$ inch plywood sheets were used for the contraction.The estimates for the main supplies used in the completion of the tunnel are included in Table 1 below.

Table 1 Estimated main supplies list for wind tunnel construction

Component Type	Quantity (est.)
Plywood Sheets (4 ft x 8 ft x 0.75 in)	10
Plywood Sheets (4 ft x 8 ft x 0.25 in)	12
Pine Struts (8 ft x 2 in x 4 in)	40
Acrylic Sheets (4 ft x 8 ft x 0.5 in)	1
Piano Hinge	1
Wood Screws (1.25 in), 3 lb box	1
Wood Screws (2 in), 3 lb box	1
Industrial Fan (48 in diameter)	1

Standard size components were cut with miter saws, table saws, and jigsaws, while more complex components, like the shape forms for the contraction section, were cut with a computer numerical control (CNC) machine (Fig. A2). Standard wood screws of varying lengths were used to secure the various components. Many other smaller components were also purchased for the tunnel, including feet, caulking material, and tape to fill gaps. Only the essential items were included in the above table.

B. Uniformity Testing Methods

Basic uniformity testing was performed on the completed tunnel. Measurements of airspeed were taken in a 9x9 evenly spaced grid across the test section, as shown below in Fig. 6. At each hole in the baseboard, measurements were taken at 9 evenly-spaced heights, to allow 81 total measurements. Baseboard holes were filled with dowel sections

when not in use. All airspeed measurements were taken with an AmProbe TMA20-HW HotWire anemometer and were recorded in ft/min and converted to ft/s.

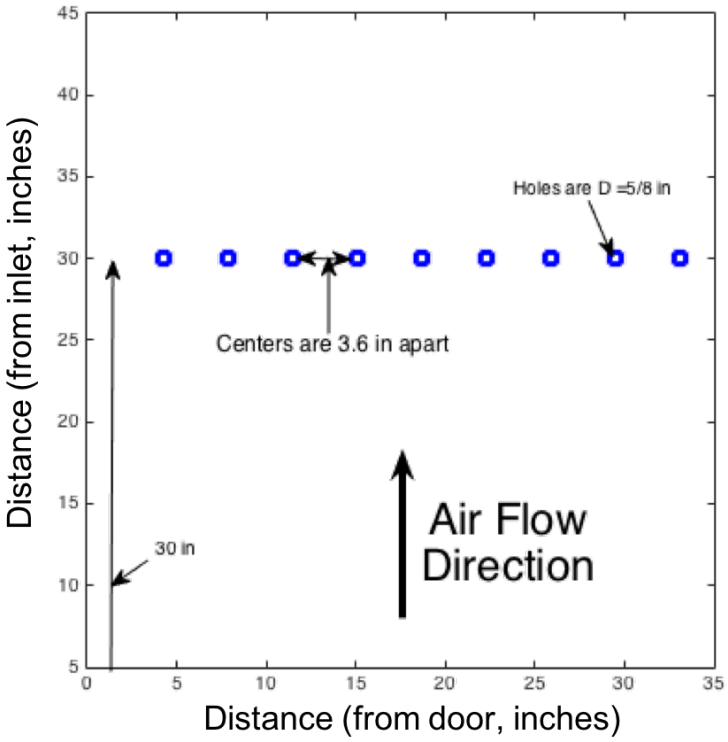

Fig. 6 Schematic diagram showing the distribution of measurement holes (blue) on the test section baseboard

In addition, the wind speed measurements at each of the 81 nodes were compared to every other node using a One-Way ANOVA method for significant differences at a confidence level of p=0.05. Further details concerning the results of the uniformity testing are included in Section 3.2.

IV. Results

The wind tunnel was built during the Fall 2017 semester, and the uniformity testing was performed early in the Spring 2018 semester. It was constructed in pieces, namely the contraction, test section, diffuser, and the fan base. The results of this build and this study are presented in the following sections. Additional pictures of the building process are presented in Fig. 12.

A. Wind Tunnel

The completed wind tunnel construct is shown in Fig. 7 below. The wind tunnel was mainly built in the AME machine shop, with completed parts transported to the OU north campus, near the Westheimer Airport (hence the lack of noise requirements). This location will be the final home of the tunnel.The manufacturing of the tunnel went according to plan and followed the design laid out in Fig. 5. The new location still doesn't have access to three-phase power, but the stock fan at full power is capable of producing wind speeds of approximately 40 ft/s in the test section. This is slightly lower than our desired test section speed of 60 ft/s. We anticipate adding an engine and powering the fan via a belt-drive in the future to produce adequate testing conditions for the UAV propellers. The dynamometer has been built by another group but has yet to be mounted to the tunnel, as of March 2018.

(a) Rear view

(b) Isometric view

Fig. 7 Images of completed wind tunnel

B. Uniformity Study Results

The uniformity study results showed a generally spatially consistent wind speed throughout the cross-section of the test section, as predicted by prior CFD testing. Analysis of the wind-speed values at each of the nodes is included in Fig. 8 below. In Fig. 8a,the wind speeds at each of the regions were mapped to a color gradient, where green was the region with the highest recorded wind speed and red was the region with the lowest recorded wind speed. In Fig. 8b, the regions with wind speed variances from mean that couldn't be accounted for by inaccuracy in the measurement device are shown, whereas in Fig. 8c the regions with wind speeds that varied significantly (based on a one-way ANOVA analysis) from the other regions are shown.

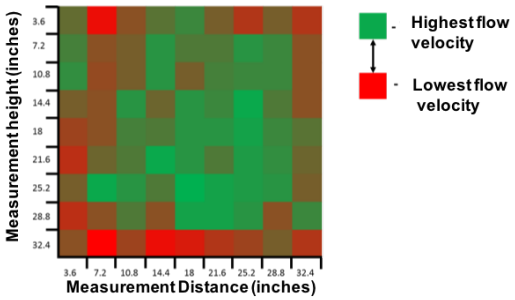

(a) Flow velocities relative to the average (81 nodes)

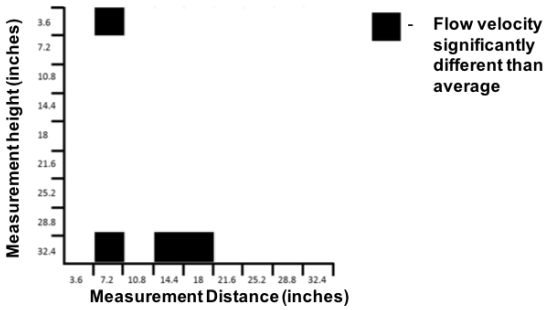

(b) Significantly different recorded velocities ($p < 0.05$)

Fig. 8 Nodal flow velocities throughout the cross-section of the wind tunnel test region

As shown in Fig. 8, four regions had readings that were significantly different than the average across all other regions. Interestingly, these regions all had recorded speeds significantly lower than the average. As expected, the lowest readings were taken near the edges of the cross-sectional area, but generally, these readings were recorded in the top and bottom rather than the sides of the testing region. We observed a fairly standard and uniform wind speed throughout the test section, as shown in Table 2, which helps to validate the use of the wind tunnel for analytical purposes.

V. Discussion

Our group built this tunnel to allow controlled testing of a variety of propellers and other aerodynamic components. Although we were not able to incorporate the dynamometer in the time allotted or use an engine to provide more

Table 2 Uniformity study flow parameters

Parameter	ft/min	ft/sec
Device Measurement Uncertainty	67.3	1.1
Average Wing Speed	2240	37.4
Standard Deviation	60	1.0
Maximum Wind Speed	2340	39.0
Minimum Wind Speed	2080	34.7
Maximum Percent Difference	4.35 %	
Minimum Percent Difference	-7.25 %	

power the fan, we were still able to verify the functionality of our tunnel under standard flow conditions, while staying well under budget. This basic and low-cost tunnel will be available to undergraduate and graduate students who have research projects to pursue in aerodynamics and will allow testing of a wide range of aerodynamic designs, because of its large 36 in by 36 in test section. It also encourages rapid development and optimization with sensors and other custom-built measurement devices, because of the ease of attachment to the wooden outer frame and the low-cost and straight forward swapping of any component of the tunnel. We hope and expect future groups to utilize and adjust this tunnel to ensure its relevance and applicability toward future aerodynamics research.

A. Study Limitations and Future Extensions

Despite the success of our project, some inaccuracies exist in the final tunnel. Specifically, because of the crude nature of wooden fabrication methods, and the complex shape of some of our plywood pieces, some gaps exist between the many plywood panels. These minor issues can be patched and mended but will likely decrease the precision and uniformity of the tunnel. In the uniformity study, the anemometer used was sensitive to rotations of the probe. Although care was taken to keep the alignment in the same direction while taking the measurements, it's possible that some rotation of the probe occurred, thus decreasing the accuracy of the device. In addition, this uniformity study was only conducted at one downstream distance within the test section. Observing uniformity in this one specific slice is no indication or proof of flow consistency throughout the entire test section, and further testing will be needed to examine the spatial uniformity of air speed with respect to this third dimension. The extensions of this project center around the implementation of a dynamometer into the tunnel and the use of an exterior engine to power the fan. However, we built the tunnel with the intention of allowing many research groups to make non-damaging and reversible modifications to the tunnel, so extensions are technically unrestrained.

B. Conclusion

Despite the project setbacks and the time that this construction took, our group managed to create a functioning wind tunnel, based on designs that we developed. We expect and believe that our work has helped to improve the OU AME department's capacity to perform valuable aerodynamics research by providing this versatile tool. In addition, we hope that our article describing the design process will be of use to researchers at other universities as they design and build similar tunnels for student research into modern aerodynamics topics.

Appendix

This appendix serves to hold extra images from the completion of the project, specifically from the design and analysis phase (Fig. 9, 10) and the construction and testing phase (Fig. 11, 12).

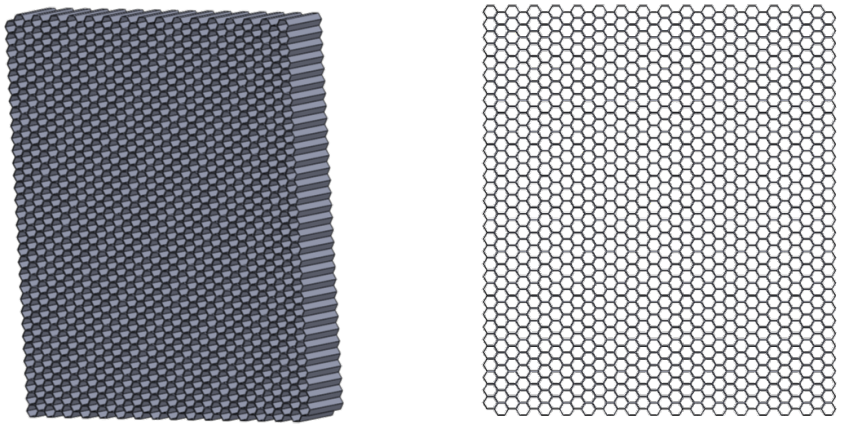

(a) Isometric view

(b) Cross-section of flow straightener

Fig. 9 CAD model of the flow straightener

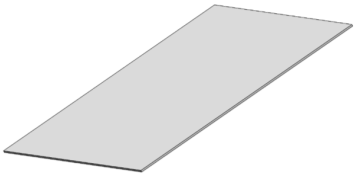

(a) CAD model of acrylic panel for test section door

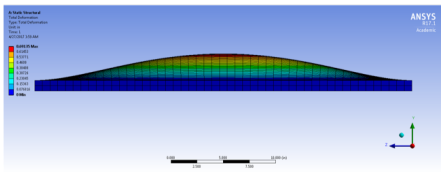

(b) FEA predicted stress on panel with applied pressure showing deformation

Fig. 10 Acrylic panel CAD and FEA analysis

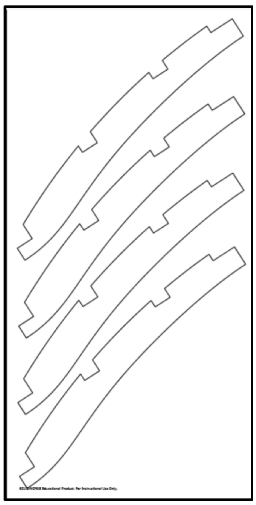

(a) Side shape forms for CNC on 4 ft by 8 ft plywood sheet

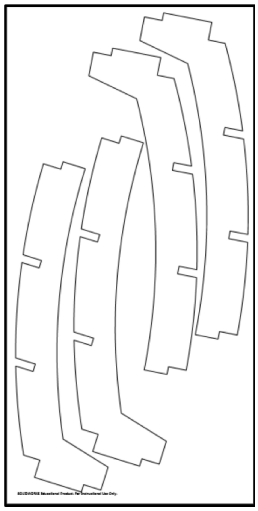

(b) Top/bottom shape forms for CNC on 4 ft by 8 ft plywood sheet

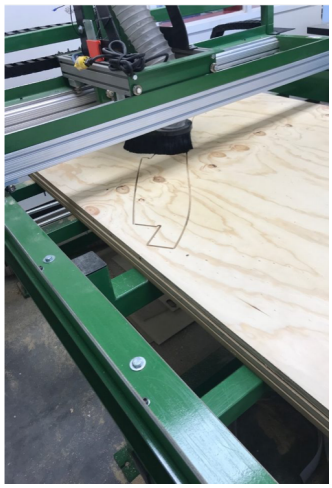

(c) Cutting the shape forms out with CNC machine at OU Innovation Hub

Fig. 11 Design and manufacturing of the shape forms for the contraction

(a) Contraction under construction

(b) Diffuser under construction

(c) Completed tunnel during testing

Fig. 12 Manufacturing and testing of the wind tunnel

Acknowledgments

The authors would like to thank the AME Machine shop, the Innovation Hub at OU, and the Rawl Engineering Practice Facility for their support and the use of their facilities during tunnel fabrication. The authors would also like to thank the Department of Aerospace and Mechanical Engineering in the Gallogly College of Engineering at the University of Oklahoma for funding this project.

References

[1] Pankhurst, R. C., and Holder, D. W., *Wind-tunnel technique: an account of experimental methods in low-and high-speed wind tunnels*, Pitman, London, UK, 1952.

[2] Rae., W. H., and Pope, A., *Low-speed wind tunnel testing*, John Wiley, Hoboken, NJ, 1984.

[3] Puri, A., "A Survey of Unmanned Aerial Vehicles (UAV) for Traffic Surveillance," *Department of Computer Science and Engineering*, 2005, pp. 1–29.

[4] Lentilhac, S., "UAV flight plan optimized for sensor requirements," IEEE, 2009, pp. 1–4.

[5] Zhang, Y., P.Tao, Liang, S., and Liang, W., "Research on application of UAV RS techniques in forest inventories," *Journal of southwest forestry university*, 2011, pp. 49–53.

[6] Xiang, H., and Tian, L., "Development of a Low-Cost Agricultural Remote Sensing System Based on an Autonomous Unmanned Aerial Vehicle (UAV)," *Journal of Biosystems Engineering*, 2011, pp. 174–190. doi:10.1016/j.biosystemseng.2010.11.010.

[7] Bristeau, P., Salaun, E., and Petit, N., "The Role of Propeller Aerodynamics in the Model of a Quadrotor UAV," 2009, pp. 683–688.

[8] "Analysis and Design of a Low Reynolds Propeller for Optimal Unmanned Aerial Vehicle (UAV) Flight," ASME, 2017.

[9] Merchant, M. P., and Miller, L. S., "Propeller Performance Measurements for Low Reynolds Number UAV Applications," Reno, Nevada, 2006. doi:10.2514/6.2006-1127.

[10] Subhas, S., Saji, V., Ramakrishna, S., and Das, H., "CFD analysis of a propeller flow and cavitation," *International Journal of Computer Applications*, 2012, pp. 49–53.

[11] Scheiman, J., "Considerations for the Installation of Honeycomb and Screens To Reduce Wind-Tunnel Turbulence," *NASA Technical Memorandum*, 1981.

[12] Scheiman, J., and Brooks, J., "Comparison of experimental and theoretical turbulence reduction from screens, honeycomb, and honeycomb-screen combinations," *Journal of Aircraft*, 1981.

[13] Hernández, M., López, A., Jarzabek, A., Perales, J., Wu, Y., and Xiaoxiao, S., *Wind Tunnel Designs and Their Diverse Engineering Applications*, InTech, Hoboken, NJ, 2013.